Iran University of Science and Technology

International Journal of

Railway Research

ISSN: 2423-3838

Investigation of goods emplacements on the derailment of the standard freight wagon in curves with dynamic simulation

Shakib Sadeghi[1], Majid Shahravi[*1]

[1]School of Railway Engineering, Iran University of Science and Technology, Tehran, Iran

ARTICLE INFO

Article history:
Received: 24.07.2023
Accepted: 19.09.2023
Published: 23.09.2023

Keywords:
Derailment
Load Placement
Open-top freight wagon
Universal Mechanism
Dynamic Simulation

A B S T R A C T

Public transportation has always been of great interest to researchers and has been considered an essential and efficient method for transporting people and various goods over the past two centuries. In recent studies, the examination of influential parameters on the efficiency of these vehicles has played a prominent role, and numerous researchers have continuously investigated the safety and various parameters of freight wagons. One of the challenges that can be raised as an issue in standard open-top freight wagons is the placement and positioning of the load inside these wagons. Considering that loading these wagons is not standardized in the industry and the load may be placed more or less in different positions at each loading stage, examining the effect of this issue on the safety of the movement of wagons in a curve can be essential. In this study, by considering a standard open-top freight wagon in the Universal Mechanism software, the effect of placing a hypothetical concentrated load in four different positions on the derailment coefficient in a curve with three different non-critical speeds is investigated. Ultimately, by comparing the results, the effect of this parameter on the derailment coefficient is discussed. The focus of this study was solely on the safety of the wagon's movement.

1. Introduction

Transporting goods via railways is a crucial aspect of the transportation industry, with different types of wagons used to carry a variety of goods. The railway system of Iran, for instance, has various types of wagons, such as flat, covered, gondola, bulk, tank, refrigerated, car-carrying, and open wagons [2]. Loading and unloading goods in these wagons is of great importance and requires careful consideration. Research has been carried out on this subject, with some studies focusing on the arrangement of wagons based on the type of goods they carry [4]. In light of recent developments, a study has been conducted on the loading of solid materials in open wagons [5]. This study proposes solutions for improving the arrangement of goods in wagons, with a particular focus on the placement of solid objects in open gondola wagons. One of the main challenges of this research is to determine whether loading goods in a wagon can directly affect the safety of the railway system. Therefore, the impact on the derailment coefficient is investigated using the Universal Mechanism software [5]. This paper aims to provide a comprehensive overview of the different types of wagons used in the Iranian railway system, the importance of loading and unloading goods, and the latest research on the placement of goods in wagons.

[*]Corresponding author
Email address: m_shahravi@iust.ac.ir

[DOI: 10.22068/ijrare.327]

2. Theory and Simulation

2.1. Preface

The derailment of railway vehicles can cause significant financial and human losses, making it crucial to prevent such incidents. The derailment of railway vehicles can be defined as the wheels leaving the track. The reasons for wheels leaving the track can be complex. Any condition that reduces the lateral stability of the track increases the risk of derailment. Typically, when a wheel experiences high lateral forces along with a decrease in vertical forces on the wheel flange, the wheel lifts off the rails, resulting in derailment. Derailments usually occur in curves where the outer rail wheels typically experience a base ratio of lateral force to vertical force (L/V or Y/Q).

2.2. An Introduction for Nadal's Derailment Criteria

The Nadal single-wheel L/V limit criterion, proposed by Nadal for French railways, has been used worldwide, including in Euro vehicle standards and the US Federal Regulations code. Nadal created the initial formula for limiting the L/V ratio to minimize the risk of derailment. Nadal assumed that the wheel was initially in point contact and that the flange point was directed towards the switch point. He concluded that the wheel moves downward relative to the rail at the flange contact point due to the rotation around the switch contact. He also proposed that a wheel lift occurs when the downward motion with saturated friction at the contact point is stopped [6].

(1)

$$F_3 = V\cos\delta + L\sin\delta = V\left(\cos\delta + \frac{L}{V}\sin\delta\right)$$
$$\begin{cases} F_2 = V\sin\delta - L\cos\delta = V\left(\sin\delta - \frac{L}{V}\cos\delta\right) & \text{when } (V\sin\delta - L\cos\delta) < \mu F_3 \\ F_2 = \mu F_3 & \text{when } (V\sin\delta - L\cos\delta) \geq \mu F_3 \end{cases}$$

The ratio of L/V can be obtained from the above equation:

$$\frac{L}{V} = \frac{\tan\delta - \frac{F_2}{F_3}}{1 + \frac{F_2}{F_3}\tan\delta} \quad (2)$$

The following equation can be obtained based on Nadal's assumption and a simple balance of forces between the wheel and the rail at a single contact point of the flange, as illustrated in Figure 1.

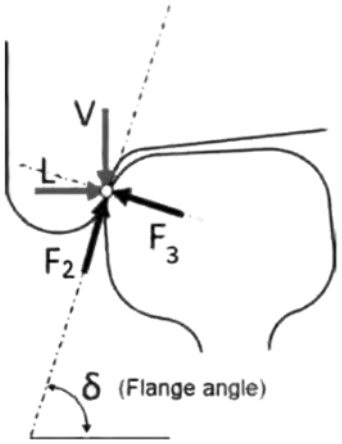

Figure 1. Schematic of forces in flange connection [6]

The well-known Nadal equation in the state of saturation, $F_2/F_3 = \mu$, has been presented in Equation 3, where μ is the coefficient of friction. This equation serves as a valuable tool for evaluating lateral and vertical forces in railway transport under various conditions.

$$\frac{L}{V} = \frac{\tan\delta - \mu}{1 + \mu\tan\delta} \quad (3)$$

2.3. Introducing the long edge open cargo wagon

The long-edged wagon is a traditional type of gondola wagon with side and end walls that have a height of more than 36 inches (44.91 cm). These wagons are primarily used to transport small materials such as coal, which do not require protection from adverse weather conditions. Long-edged wagons are categorized into three groups based on their design and usage. The first group are tub-shaped wagons, which have a long edge and no drain valves. In the latter half of the 20th century, these wagons were used to transport more coal per wagon. Unlike hopper wagons, tub-shaped wagons do not have equipment to open and close drain valves, allowing them to carry a larger volume of cargo. The emptying process of these wagons involves the use of a "Rotary Car Damper" mechanism, which keeps the wagon firmly in place while rotating it to empty its contents from the top. The second group are long-edged wagons with floor drains. These wagons have a movable floor that functions as an emptying

[DOI: 10.22068/ijrare.327]

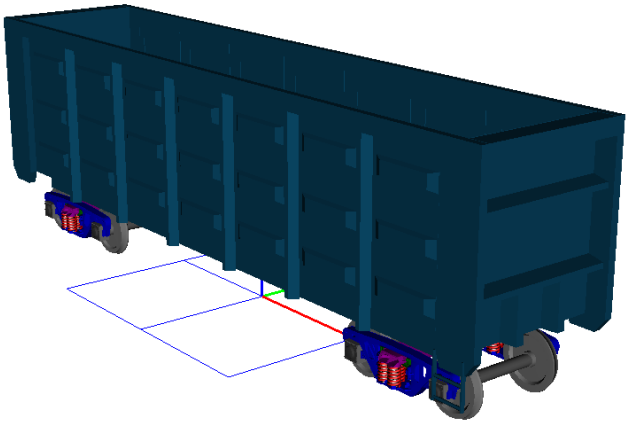

Figure 2. Schematic of the model created using Universal Mechanism software.

valve. When the wagon is emptied, the contents are released between two rails. The third group consists of long-edged wagons with side doors. These wagons are emptied through doors built into their side walls. To empty the contents, the wagon must be placed on a platform, and appropriate equipment must be used to guide the contents to the bottom of the platform. Overall, the long-edged wagon is a versatile type of gondola wagon that offers different designs and usage options. Its ability to transport small materials, such as coal, with ease makes it an important component of the transportation industry. According to the Nadal assumption and a simplified equilibrium of forces between the wheel and rail at a single point of contact on the flange, as illustrated in Figure 1, the following equation can be derived. This equation serves as a basis for further analysis and evaluation of lateral and vertical forces in railway transport [1].

The long-edged wagon is a suitable means of transportation for bulky and heavy raw materials, stones, minerals, and packaged loads. The wagon carrier's metal parts are fabricated from St 52-3 or equivalent materials. The wagon's floor plate is composed of St 52-3 steel plate and is 6 mm thick. To access the wagon's interior, a ladder is installed on the end wall. The wagon is equipped with an automatic coupler that has a reversible stroke of 110 mm and an energy absorption capacity of 60 kilojoules. As an alternative option, the Bogie 18-100 can be used along with the Russian brake system. The wagon design conforms to the EN standard, and the UIC guidelines are implemented for RIV utilization [7].

Figure 2 depicts the open cargo wagon modeled in the software, while Figure 3 and Table 1 present its dimensions and other specifications.

Table 1. Specifications of the long-edged open cargo wagon [8]

Feature	Spec.
Axel load	Maximum 22.5 tons
Line width	1435 Millimeters
Brake system	Knorr
Maximum full/empty speed	120/100 Kilometers per hour
Minimum rail curve radius	75 Meters
Coupling system	Automatic SA3
Wagon length	14240 Millimeters
Wagon width	2950 Millimeters
Bogie	18-100
The distance between two bogies	9000 Millimeters

[DOI: 10.22068/ijrare.327]

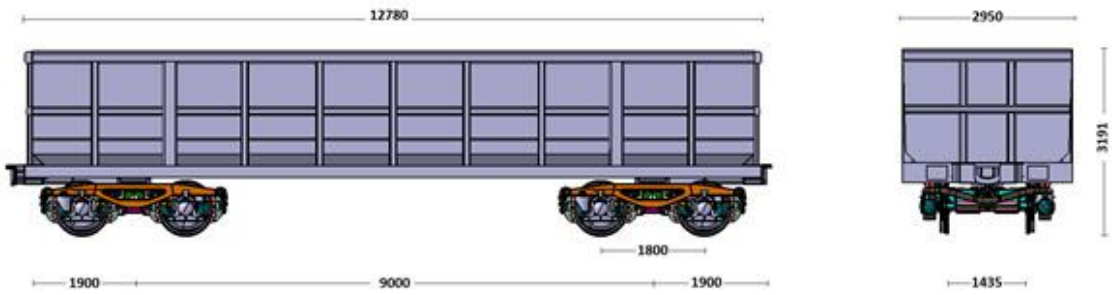

Figure 3. Specifications of the long-edged open cargo wagon[8]

Four models have been included to place the load in this wagon. It is worth mentioning that in this research, it is assumed that the load is fixed and restrained inside the wagon in such a way that it does not move. The description of what was said is shown in Figure 4.

The fifth load placement model is an automated model in which the load is applied to the wagon body. The permissible load for each wagon is assumed to be 90 tons, with the wagon body weighing approximately 20 tons and the load weighing 70 tons.

2.4. Introducing the designed path in UM software

In railway engineering, horizontal curves are typically represented using curve radius (R) or curve curvature (1/R). In some countries, the curve radius (R) is expressed as the angle in degrees of a 100-foot (30.48-meter)-long curve [8]. For simulation purposes, a line with the specifications provided in Table 2 has been prepared.

Table 2. Path specifications in UM software

Parameter	Symbol	Value
The stable length of the curve	S	200 (m)
Curve radius	R	190 (m)
Around	h	0.09 (m)
The entire length of the route	L	300 (m)

Figure 5 presents a schematic view of the path created in the software in the form of a curve.

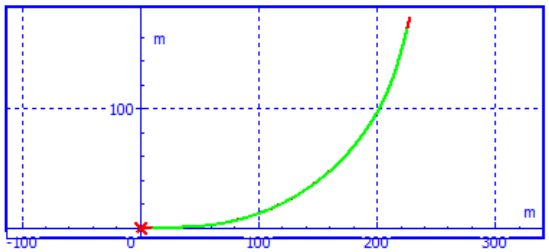

Figure 5. Schematic of the path created in UM

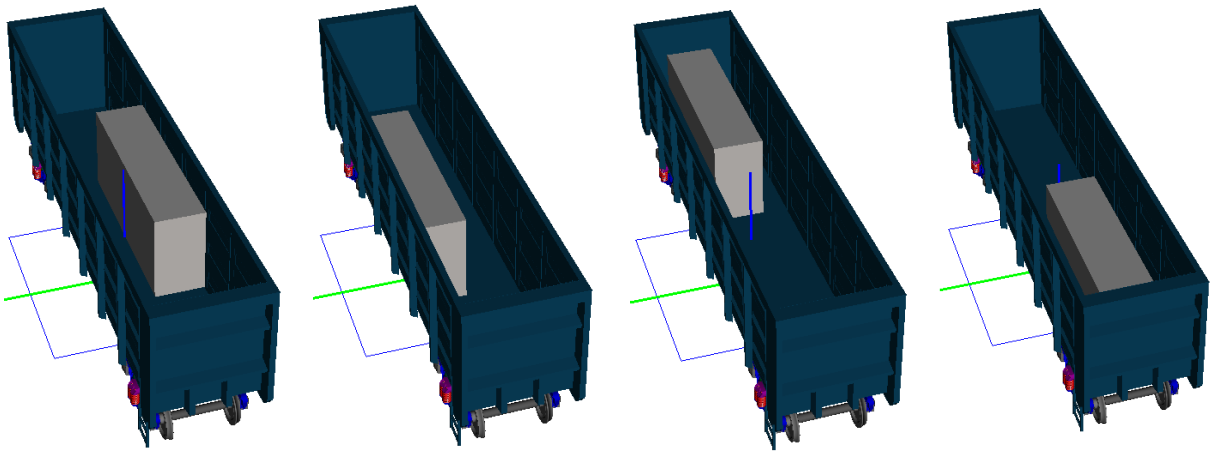

Figure 4. The load placement models for the long-edged open cargo wagon include: a) the middle and back of the wagon, b) the middle and front of the wagon, c) the left side of the wagon, and d) the right side of the wagon

[DOI: 10.22068/ijrare.327]

In accordance with reference [7], the long-edged wagon is permitted to travel at speeds of up to 80 km/h without a load and 100 km/h with a load. To analyze the performance of each load placement model, speeds of 10 m/s, 15 m/s, and 20 m/s were applied. Figure 6 provides a view of the wagon and the route modeled in the software.

3. Simulation results

In the preceding section, a comprehensive evaluation of various wagon models was conducted on a predetermined route at fixed speeds. This section presents the diagrams obtained from the modeling process. It is noteworthy that the axes of these diagrams are calibrated from the front of movement path number one to the rear of movement path number four. This indicates that the route under consideration comprises four distinct movement paths, and each wagon model's performance was evaluated on each of these paths. The diagrams offer a visual representation of the performance of each wagon model along the length of the route, facilitating a thorough analysis of their respective merits and demerits.

3.1. Evaluation at v= 10 m/s

Initially, the graphs of each wheel in every wagon were examined, and the wheel with the highest Y/Q coefficient was identified as the critical wheel. An exemplar of the diagram depicting all the wheels of a wagon is illustrated in Figure 7.

As illustrated in Figure 7, the Y/Q ratio graph of the right wheel's axis number one exhibits the highest values, thus qualifying it as the critical wheel in this case. Using the same methodology, the critical wheel and axle were identified in other wagons. Table 3 reports the highest Y/Q coefficient value obtained for a wagon traveling at a speed of 10 m/s using this approach.

Table 3. Identification of critical wheel and axle based on load placement type at 10 m/s

The type of load placement in the wagon	Critical wheel and axle
Load in the back of the wagon (in short ModelB)	Axle number 1 right wheel
Load in the front part of the wagon (in short ModelF)	Axle number 3 right wheel
Load on the left side of the wagon (in short ModelL)	Axle number 3 right wheel
Load on the right side of the wagon (in short ModelR)	Axle number 1 right wheel
Distributed load on the body of the wagon (in short Model)	Axle number 1 right wheel

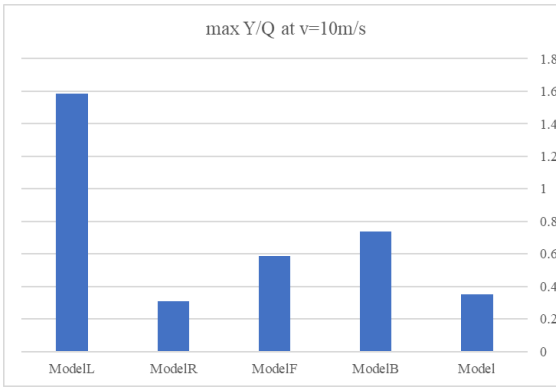

Figure 8. Comparison of maximum Y/Q ratios for wagons at v= 10 m/s

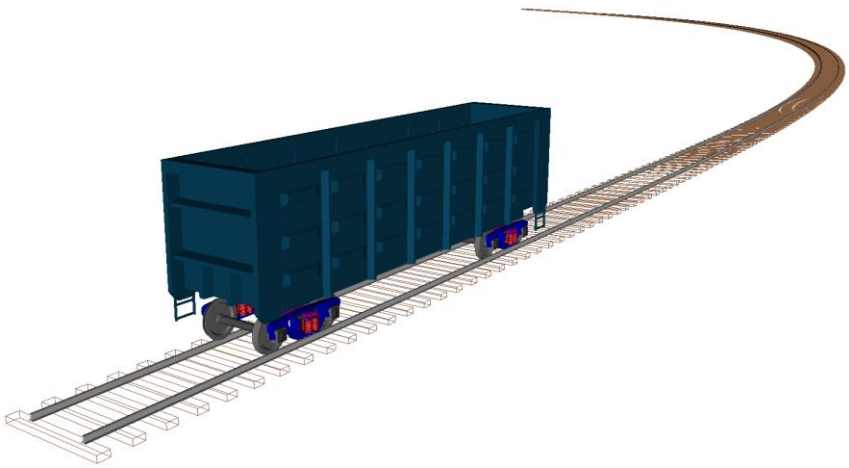

Figure 6. A view of the wagon and path modeled in UM

[DOI: 10.22068/ijrare.327]

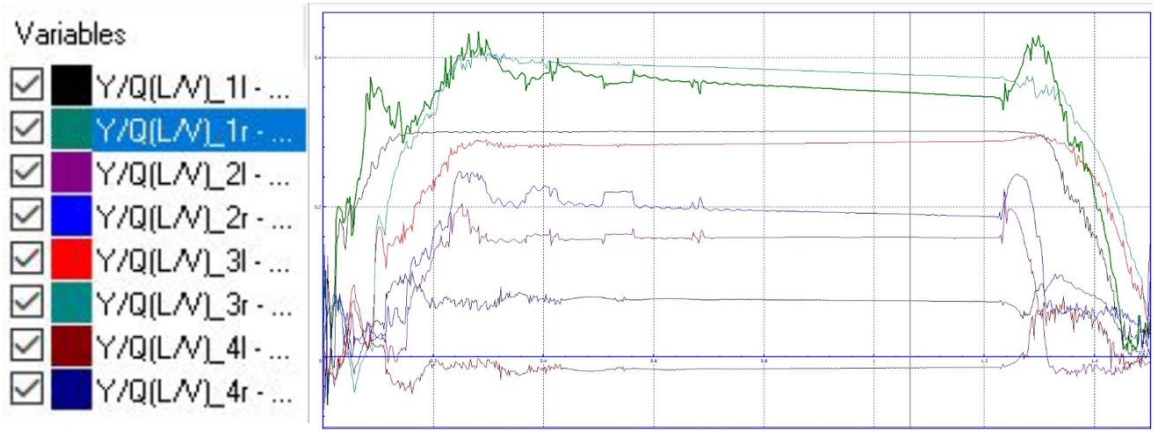

Figure 7. Y/Q ratio diagram for a rear-loaded wagon at 10 m/s.

Figure 8 presents a comparison chart of Y/Q ratios for wagons with the aforementioned loading types. It should be noted that through multiple repetitions of the simulation, the cargo wagon located on the left side experienced derailment at a speed of 10 m/s, thus failing to complete the designated route.

3.2. Evaluation at v= 15 m/s

Applying the methodology outlined in Section 1-3, Table 4 presents the critical wheel and critical axle identified at a speed of 15 m/s. Furthermore, Figure 9 illustrates the highest recorded Y/Q coefficient value for each wagon traveling at a speed of 15 m/s.

Table 4. Identification of critical wheel and axle based on load placement type at 15 m/s

The type of load placement in the wagon	Critical wheel and axle
Load in the back of the wagon (in short ModelB)	Axle number 1 right wheel
Load in the front part of the wagon (in short ModelF)	Axle number 3 right wheel
Load on the left side of the wagon (in short ModelL)	Axle number 1 right wheel
Load on the right side of the wagon (in short ModelR)	Axle number 4 right wheel
Distributed load on the body of the wagon (in short Model)	Axle number 1 right wheel

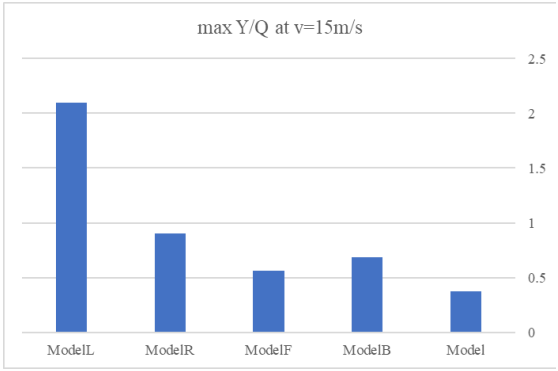

Figure 9. Comparison of maximum Y/Q ratios for wagons at v= 15 m/s

3.3. Evaluation at v= 20 m/s

Applying the methodology outlined in Section 1-3, Table 5 presents the critical wheel and axle identified at a speed of 20 m/s. Furthermore, Figure 10 illustrates the highest recorded Y/Q coefficient value for each wagon traveling at a speed of 20 m/s.

Table 5. Identification of critical wheel and axle based on load placement type at 20 m/s

The type of load placement in the wagon	Critical wheel and axle
Load in the back of the wagon (in short ModelB)	Axle number 1 right wheel
Load in the front part of the wagon (in short ModelF)	Axle number 3 right wheel
Load on the left side of the wagon (in short ModelL)	Axle number 1 right wheel
Load on the right side of the wagon (in short ModelR)	Axle number 4 left wheel
Distributed load on the body of the wagon (in short Model)	Axle number 1 right wheel

[DOI: 10.22068/ijrare.327]

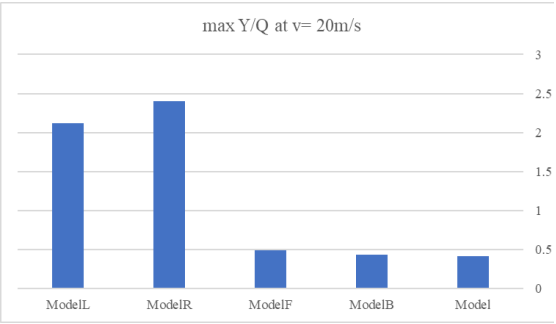

Figure 10. Comparison of maximum Y/Q ratios for wagons at v= 20 m/s

4. Discussion, conclusions and suggestions

Before delving into the results, it is essential to consider some key points that were raised in earlier sections. Of particular note, it is important to recognize that changes in the placement of the load within wagons can have a significant impact on their safety. While the investigation of Nadal's relation index in derailment has provided some evidence of its effectiveness, the present study has identified several challenges associated with this index that merit careful consideration. With that said, the results of this study can be broadly categorized into three main areas, which are discussed in detail in the following sections. By carefully analyzing and interpreting these findings, it is possible to gain a deeper understanding of the factors that influence the performance and safety of wagons under different loading and speed conditions.

4.1. Maximum values of Nadal index

The results of this study provide critical insights into the complex and multifaceted nature of wagon safety. By applying the methodology outlined in Section 3, the critical wheel and axle were identified for speeds of 10 m/s, 15 m/s, and 20 m/s. The comparison of Y/Q ratios for wagons with different loading types at 10 m/s revealed that the Y/Q ratio of the right wheel's axis number 1 exhibited the highest values, qualifying it as the critical wheel in this scenario. A similar approach was taken for speeds of 15 m/s and 20 m/s.

Furthermore, the investigation of Nadal's index in derailment yielded some evidence of its effectiveness. However, the study also identified several challenges associated with this index. Specifically, the maximum ratio of the Nadal index for ModelL compared to ModelR at a speed of 10 m/s was approximately 5.16 times, underscoring the critical role that load placement plays in wagon safety. Table 6 provides a more comprehensive breakdown of the ratios between the maximum Nadal index for different models at the modeled speeds.

Overall, the findings of this study can be categorized into three main areas: the identification of critical wheels and axles based on load placement type, the comparison of Y/Q ratios for wagons with different loading types, and the examination of Nadal's index in derailment. By carefully analyzing and interpreting these results, it is possible to develop more effective strategies for improving wagon design and mitigating safety risks associated with derailment.

Table 6. Maximum Y/Q ratio based on load placement type in wagons

Different models of load placement	Maximum Y/Q ratio
V=10m/s	
Maximum ratio (ModelL) to (ModelF)	2.7
Maximum ratio (ModelL) to (ModelB)	2.15
Maximum ratio (ModelL) to (ModelR)	5.16
Maximum ratio (ModelL) to (Model)	4.5
V=15m/s	
Maximum ratio (ModelL) to (ModelF)	3.75
Maximum ratio (ModelL) to (ModelB)	3.08
Maximum ratio (ModelL) to (ModelR)	2.32
Maximum ratio (ModelL) to (Model)	5.6
V=20m/s	
Maximum ratio (ModelL) to (ModelF)	4.35
Maximum ratio (ModelL) to (ModelB)	4.88
Maximum ratio (ModelL) to (ModelR)	0.88
Maximum ratio (ModelL) to (Model)	5.08

The results of this study indicate that Nadal's index is significantly higher when the load is placed on the side of the curve as opposed to when it is applied to the body. Specifically, this

[DOI: 10.22068/ijrare.327]

index is up to five times larger on average in the former scenario, which considerably increases the risk of derailment. Conversely, loading in the back and front of the wagon, as opposed to the sides, at different speeds results in a Nadal index that is less than half in the critical state. This finding suggests that by adhering to this simple guideline, the risk of derailment can be significantly reduced by more than 50%.

Moreover, as the speed of the train increases, the Nadal ratio for loading on the side of the curve and opposite to the curve approaches one. This observation suggests that the risk of derailment is significant in both cases, and at high speeds, the rule of low speed is not established. These findings highlight the critical role that load placement plays in wagon safety and provide valuable insights into the factors that impact derailment risk. By carefully analyzing and interpreting these results, it is possible to develop more effective strategies for improving wagon design and mitigating safety risks associated with derailment.

4.2. Investigating the Impact of Speed on Preventing Wagon Derailment

As discussed in Section 3, loading in the same direction as the curve results in a significantly higher derailment index at the critical points for the wheel and axle. However, it is important to note that the simulation in the software utilized several simplifying conditions, disregarding the effects of many physical phenomena and assuming ideal conditions. Nevertheless, at a speed of 10 m/s, compared to speeds of 15 m/s and 20 m/s, the loaded in the same direction as the curve experienced a higher derailment risk.

To further investigate this issue, the tables and graphs obtained from the software were analyzed. It was observed that the time the train spent in a critical state, as indicated by the Nadal index, had a significant effect on the derailment. This was because, as the speed of the train increased, the distance traveled remained constant, resulting in a decrease in the time of passing. This phenomenon has also been noted in other indexes that incorporate the time of passing in a critical state as a less conservative criterion than the Nadal index.

However, this issue is beyond the scope of this research. Therefore, further investigations are needed to explore this topic in depth. Nevertheless, the findings of this study provide critical insights into the factors that impact wagon safety and highlight the need for continued research and development in this area.

4.3. Analysis of Critical Failure of Wheels and Axles Based on Speed and Load Placement

The impact of load placement and speed on the criticality of the wheel and axle in wagon derailment is a critical factor to consider in wagon design and safety. However, the lack of simulation models limits the in-depth analysis of this study. Nevertheless, the comparison of Table 3 for a wagon with a load in the front part to the right part revealed a shift in the critical wheel and axle from the right wheel axel No.4 to the left wheel axel No.1. Moreover, a comparison of Table 3 with Tables 4 and 5 for the wagon with a load on the right side (ModelR) demonstrated that as the speed increased from 10 m/s to 15 m/s and 20 m/s, the critical wheel and axle shifted from the left wheel axel No.4 to the left wheel axel No.4.

These observed changes in criticality due to load placement and speed can have significant implications for wagon design and safety. Even a small change in load placement can result in a significant shift in the critical wheel and axle, which can impact the overall stability of the wagon and increase the risk of derailment. Similarly, the observed changes in criticality due to speed highlight the importance of considering speed as a critical factor in wagon design and safety. By carefully analyzing and interpreting these findings, it may be possible to develop more effective strategies for improving wagon design and mitigating safety risks associated with derailment.

However, it is essential to acknowledge that these findings are limited by the simplifying conditions used in the simulation models employed in this research. Future studies should consider more complex simulation models that incorporate a wider range of physical phenomena to provide a more comprehensive understanding of the factors that impact wagon safety. Despite these limitations, the findings of this study provide valuable insights into the factors that impact wagon safety and underscore the need for continued research and development in this area.

[DOI: 10.22068/ijrare.327]

References

[1] G. Aghajanai, M. Talei-Nouri, and M. Maki, "Introduction to railway freight cars," Tehran: Taher Cultural and Artistic Institute, 1387.

[2] P. Swamidas K, "Progress in Railroad Freight Car Engineering," in ASME 1997 International Mechanical Engineering Congress and Exposition, Dallas, 2022.

[3] S. P. Mineyev, A. A. Prusova, M. A. Vygodin, and A. S. Mineyev, "The main technological solutions for the effective discharge of the frozen cargo from gondola car," Bulletin of Dnipropetrovsk National University of Railway Transport V. Lazaryan, no. 40, pp. 124-130, 2012.

[4] O. Lavrukhin, A. Kovalov, D. Kulova, and A. Panchenko, "Formation of a model for the rational placement of cars with dangerous goods in a freight train," Procedia Computer Science, vol. 149, pp. 28-35, 2019.

[5] A. Scherbakov, M. Lunyakov, V. Smirnov, V. Kaigorodova, and N. Verbova, "Options for placement and transport of bulk goods by rail," Transportation Research Procedia, vol. 63, pp. 1498-1504, 2022.

[6] S. Iwnicki, M. Spiryagin, C. Cole, and T. McSweeney, Handbook of Railway Vehicle Dynamics, Taylor & Francis, 2019.

[7] "Freight Wagon Mineral Type," Gpig-co.com. [Online]. Available: https://www.gpig-co.com/freight-wagon-mineral-type/. ↗ [Accessed: Jul. 23, 2023].

[8] S. V. Myamlin, I. U. Kebal, and S. R. Kolesnykov, "Design review of gondola car," Science and Transport Progress, vol. 6, no. 54, pp. 136-145, 2014.

[9] S. Iwnicki, M. Spiryagin, C. Cole, and T. McSweeney, Handbook of Railway Vehicle Dynamics, Taylor & Francis, 2019.

[10] "IRICO," Iri.co.ir. [Online]. Available: http://it.iri.co.ir/web/high_side.aspx. ↗ [Accessed: Jul. 23, 2023].

[11] C. Esveld, Modern Railway Track, MRT-Productions, 2015.

[DOI: 10.22068/ijrare.327]